Theoretical study on the mechanism of CH 3 NH 2 and O 3 atmospheric reaction

2 **AUTHORS**, INCLUDING:

Morteza Vahedpour
University of Zanjan

45 PUBLICATIONS   **185** CITATIONS

Theoretical study on the mechanism of CH_3NH_2 and O_3 atmospheric reaction

SAMIRA VALEHI and MORTEZA VAHEDPOUR*

Department of Chemistry, University of Zanjan, P O Box 45371-38791, Zanjan, Iran
e-mail: vahed@znu.ac.ir

Abstract. Reaction pathways of methylamine with ozone on the singlet potential energy profile have been investigated at the RB3LYP/6-311++G (3df–3pd) computational level. Calculated results reveal that six kinds of products P_1 ($CH_3NO + H_2O_2$), P_2 ($CH_3NH + OH + O_2$), P_3 ($NH_2CH + HO_2+ OH$), P_4 ($CH_2NH + H_2O +O_2$), P_5 ($NH_2CH_2OH + O_2$), P_6 ($NH_3+ CH_2O +O_2$) are obtained through variety of transformation of one reactant complex C1. Cleavage and formation of the chemical bonds in the reaction pathways have been discussed using the structural parameters. Based on the calculations, the title reaction leads to $NH_3+ CH_2O + O_2$ as thermodynamic adducts in an exothermic process by -76.28 kcal/mol in heat realizing and spontaneous reaction by -86.71 kcal/mol in standard Gibbs free energy. From a kinetic viewpoint, the production of $CH_3NH + OH + O_2$ adducts with one transition state is the most favoured path.

Keywords. Ozone; calculation; reaction mechanism; potential energy profile; transition state.

1. Introduction

Methylamine is the simplest primary amine. It is very important in organic syntheses, biological process and atmospheric process.[1] Methylamine is prepared commercially by the reaction of ammonia with methanol in the presence of a silicoaluminate catalyst.[2] The oxidation chemistry of the methylamine has been presented in fuels contributions to NOx emissions from practical combustion devices. Methylamine oxidation chemistry has been down in fuel to production of NO_x. First, methylamine is converted to HCN and NH_3, then these two species can be oxidized to NO_x.[3–5]

Methylamine's production and use as an intermediate in the synthesis of pharmaceuticals, pesticides, solvents, explosives, surfactants, and photographic developers may result in its release to the environment through various waste streams. If released to air, vapour pressure of 2650 mm Hg at 25°C indicates that methylamine will exist solely as a gas in the atmosphere. Gasphase methylamine will be degraded in the atmosphere by reaction with photochemically produced hydroxyl radicals; the half-life for this reaction in air is estimated to be 18 h. Gas-phase methylamine is degraded in the atmosphere by reaction with ozone; the half-life for this reaction in air is estimated to be 540 days.[6] Methylamine does not contain chromophores that absorb at wavelengths >290 nm and therefore is not expected

to be susceptible to direct photolysis by sunlight.[7] There are many experimental and theoretical studies on the different aspects of methylamine such as quantum chemical parameters and spectroscopic properties.[8–12] Several theoretical studies have also been devoted to the reaction of CH_3NH_2 with OH[4], HNO_2[13], HS[14], CO_2[15] and so forth using the density functional theory or the *ab initio* methods.

Methylamine is released in different ways into the atmosphere and will have devastating effects on animals and the atmosphere. In this study, we carry out theoretical studies on the singlet potential energy profile, PEP, for the mechanism of $CH_3NH_2+ O_3$ reaction to find a way to eliminate methylamine from the atmosphere. Our main aim is to reveal the details of the reaction mechanism to explain the formation of products and provide further information about reaction of $CH_3NH_2+ O_3$ on the singlet potential energy surface.

2. Computational Details

All the calculations are performed with the Gaussian-03 program.[16] Geometrical parameters of the reactants, products, intermediates (denoted as INs) and transition states (denoted as TSs) involved in the $CH_3NH_2+O_3$ reaction are fully optimized using DFT with the restricted Becke 3-parameter hybrid exchange[17] and Lee–Yang–Parr[18] correlation density functional (RB3LYP) in conjunction with the 6-311++G(3df–3pd) basis

*For correspondence

set. Vibrational frequencies were obtained for the verification of the optimized geometries. Any reactant, product intermediate possesses all real frequencies and any transition state has only one imaginary frequency. These frequencies are without any scaling factors. Connection between reactants, intermediates, transition states and products are confirmed by intrinsic reaction coordinate, IRC, analysis at the RB3LYP level. To improve the accuracy of energetic information on minimum energy path (MEP), a higher level of electronic correlation method, CCSD/6-311++G (3df–3pd) is employed in the singlet point energy calculations. Topological analysis was carried out with AIM2000 program[19] and molecular graphs in the reaction pathway of CH_3NH_2 and O_3 were plotted.

3. Results and Discussion

Optimized geometrical parameters of the reactants (R), intermediates (INs), transition states (TSs) and products (Ps) involved in the $CH_3NH_2 + O_3$ reaction are shown in figure 1. To simplify our discussion, the energy of reactants, $CH_3NH_2 + O_3$, is set to be zero for reference. Total energies and relative energies of all species have been listed in table 1. The calculated vibrational frequencies at the RB3LYP level are listed in table 1S (supporting information). Results show that all intermediates are true minima on the reaction potential energy surface, and any transition state has only one imaginary frequency. Finally, by means of transition states and their connected intermediates or products at the RB3LYP level, a schematic PEP for $CH_3NH_2 + O_3$ reaction on the singlet potential energy profile is plotted in figure 2. Singlet surfaces are represented by solid lines and relaxation singlet to triplet at the end of reaction mechanism are represented by dashed lines.

3.1 *Initial association on the singlet potential energy surface*

All the elementary reactions in this study begin with the formation of a pre-reactive complex that is marked by C1. This complex has a four-membered ring structure with Cs molecular symmetry. It is formed when the nitrogen atom in methylamine molecule approaches the terminal atoms of ozone molecule without entrancing any energy barrier. Formation of ring structure and newly bonds are also confirmed by atoms in molecules (AIM) topological analysis of the wave functions. The details of AIM results are shown in figure 3. Bond length of 8N–10H in C_1 is 1.010 Å, which is about

0.003 Å shorter than the parent CH_3NH_2 molecule. Negative charge is transferred to the nitrogen of methylamine from oxygen of ozone. Therefore, negative charge of nitrogen is increased. Consequently, absorption of positive charge by nitrogen increased and this makes the length of N-H bond shorter and stronger. Newly formed bonds length of 8N-2O and 8N-3O are 2.931, 2.781 Å, respectively. C_1 energy is 11.35 kcal/mol less than the original reactants and no transition state has been found for the formation of reactant to $CH_3NH_2-O_3$ complex. From variation of the initial complex, six kinds of products are obtained via different pathways. Details of the reaction mechanism on the singlet potential surfaces are discussed below.

3.2 *Isomerization and dissociation pathways*

Our calculations led to the identification of one reactant complex for the reaction between CH_3NH_2 and O_3 on the singlet potential energy surfaces. From the variation of the reactant complex, six kinds of products are obtained, which can be summarized in scheme 1.

C1 stands for the initial complex and the final products are defined as P_1 ($CH_3NO + H_2O_2$), P_2 ($CH_3NH + O_2 + OH$), P_3 ($NH_2CH + HO_2 + OH$), P_4 ($CH_2NH + H_2O + O_2$), P_5 ($NH_2CH_2OH + O_2$) and P_6 ($NH_3 + CH_2O + O_2$).

3.2a *Formation pathway of P_1 ($CH_3NO + H_2O_2$):*
There is only one pathway to reach P_1 as final product.

PathP$_1$: $R \rightarrow C1 \rightarrow IN1 \rightarrow IN3 \rightarrow CP_1 \rightarrow P_1$

In path P_1, in the first step, the initial reactant complex C1 is formed. C1 complex has a four-membered ring structure that is 11.35 kcal/mol stable than the original reactants. C_1 ($CH_3NH_2-O_3$) undergoes 8N-10H bond rupture and 10H-2O and 8N-3O bond formation to transform into IN1 via TS1 with an energy barrier of 19.08 kcal/mol. Obtained transition state has a five-membered ring structured that is 12.62 kcal/mol unstable than original reactants. This structure is formed when the O1 and O3 atoms of ozone approach nitrogen atom of CH_3NH_2 molecule. Imaginary frequency of TS1 is 594i cm^{-1} using RB3LYP method in the reaction coordinate. Then, IN1 is transformed into IN3 via TS2 with an energy barrier of 72.60 kcal/mol. Imaginary frequency of TS2 is 1585i cm^{-1}. IN3 as an intermediate is transformed into the CP_1 via TS3 with an imaginary frequency of 356i cm^{-1} in the reaction pathway. The energy barrier for IN3→CP$_1$
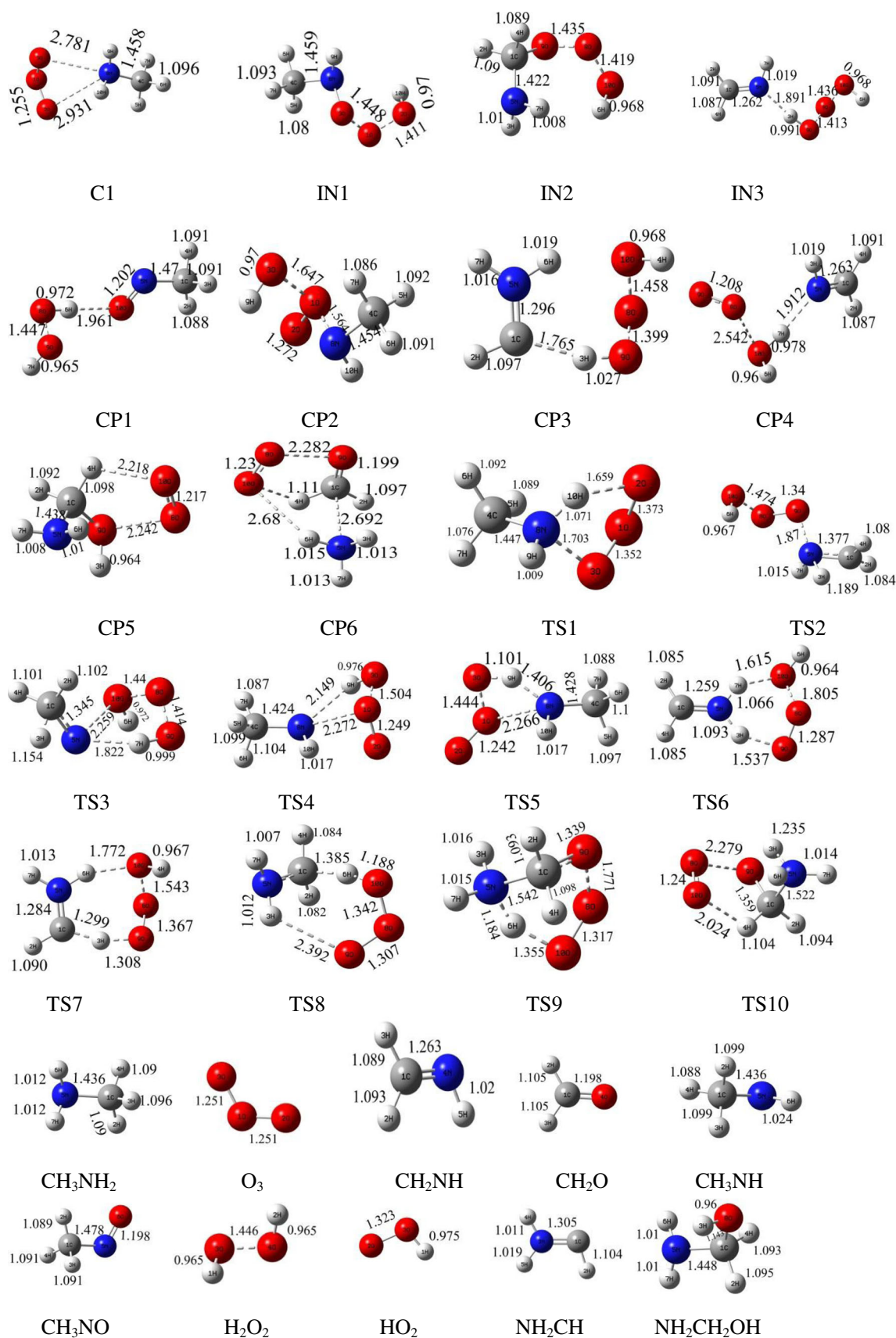
Figure 1. Geometries of reactants, products, intermediates and transition states optimized on the singlet PEP at the RB3LYP level (bond distances are in angstrom).

Table 1. Total energies, relative energies (in parentheses) and ZPE of the reactants, products, intermediates and transition states in the $CH_3NH_2+O_3$ reaction on the singlet PEP.

Species	RB3LYP	ZPE	CCSD(T)
Reactants	−321.3282(0.00)	0.0711	−320.8196(0.00)
C1	−321.3329(−2.92)	0.0725	−320.8377(−11.35)
IN1	−321.3611(−20.94)	0.0748	−320.8658(−28.99)
IN2	−321.4106(−51.94)	0.0715	−320.9145(−59.55)
IN3	−321.3961(−42.60)	0.0725	−320.8983(−49.38)
CP1	−321.4104(−51.58)	0.0715	−320.9853(−60.05)
CP2	−321.3013(16.87)	0.0728	−320.8067(8.09)
CP3	−321.3521(−14.99)	0.0727	−320.8537(−21.39)
CP4	−321.3961(−42.60)	0.0692	−320.9051(−53.65)
CP5	−321.4028(−46.81)	0.0740	−320.9156(−60.24)
CP6	−321.3984(−44.08)	0.0695	−320.8954(−47.56)
TS1	−321.3081(12.61)	0.0728	−320.8072(7.78)
TS2	−321.2581(43.97)	0.0679	−320.7501(43.61)
TS3	−321.2633(40.72)	0.0676	−320.7575(38.96)
TS4	−321.2737(34.19)	0.0702	−320.7992(12.80)
TS5	−321.2800(30.24)	0.0672	−320.7914(17.69)
TS6	−321.3603(−20.14)	0.0692	−320.8547(−22.02)
TS7	−321.3508(−14.18)	0.0684	−320.8672(−29.86)
TS8	−321.3146(8.53)	0.0680	−320.8128(4.26)
TS9	−321.3694(−25.83)	0.0724	−320.8808(−38.40)
TS10	−321.3538(−16.06)	0.0703	−320.8570(−23.46)
P1	−321.4058(−48.69)	0.0697	−320.9102(−56.85)
P2	−321.3141(8.84)	0.0609	−320.8083(7.09)
P3	−321.2833(28.17)	0.0622	−320.8436(15.06)
P4	−321.4491(−71.94)	0.0567	−320.9476(−80.32)
P5	−321.4617(−83.77)	0.0730	−320.9203(−63.18)
P6	−321.4476(−74.92)	0.0644	−320.9455(−79.00)

Total energy and ZPE are in Hartree and relative energy is in kcal/mol.
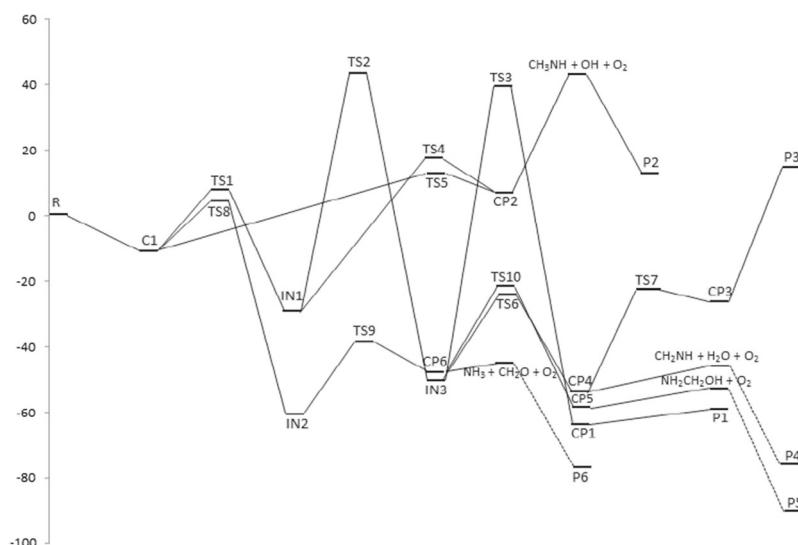
Figure 2. Calculated potential energy profile of $CH_3NH_2+O_3$ reaction at RB3LYP level of computation.

conversion is 88.34 kcal/mol. CP_1 is 60.05 kcal/mol stable than original reactants. CP1 is the complex between H_2O_2 and CH_3NO which are indicated by the bond of 6H-10O. It can be directly decomposed to H_2O_2 and CH_3NO by 6H-10O bond rupture without any transition state.
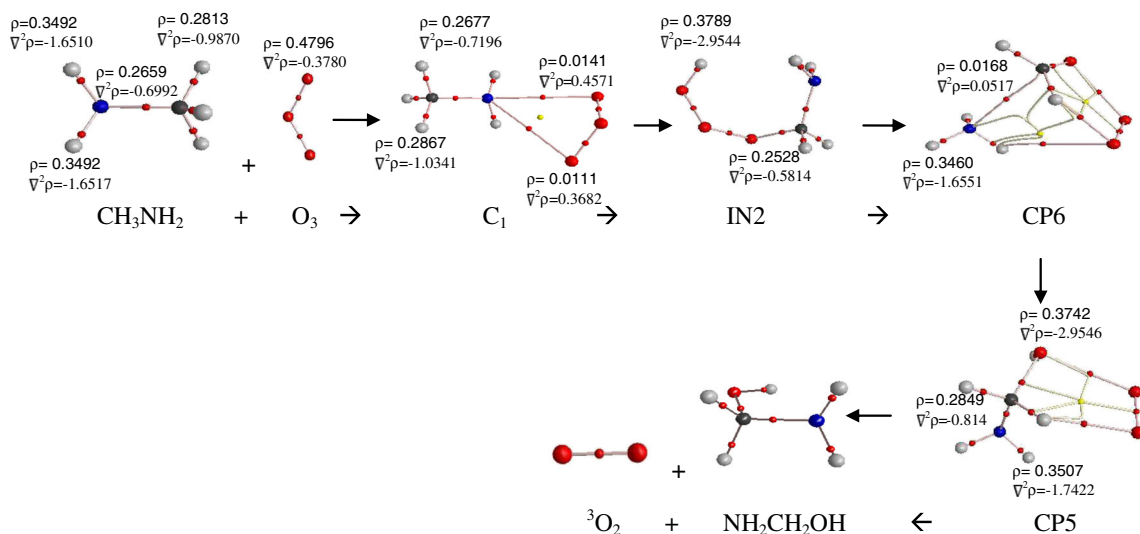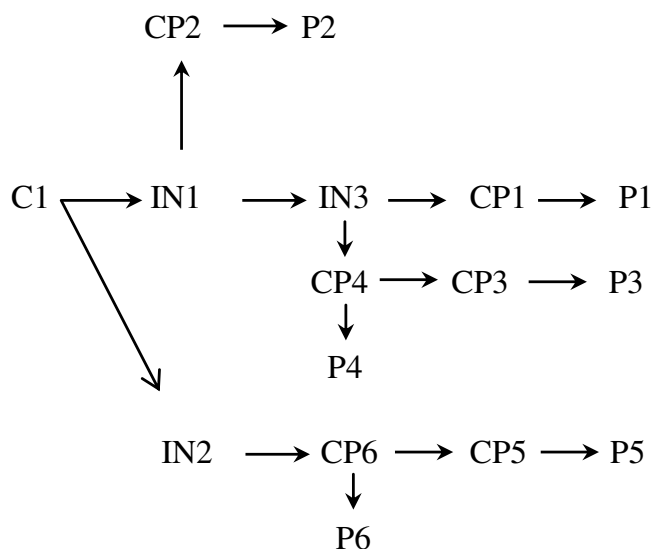
Figure 3. AIM molecular graphs of CH$_3$NH$_2$+O$_3$ for path P5 (small yellow circle represents ring critical point and small red circle with connection to atoms represents bond critical point).

Scheme 1. Relationship among the reactant complex and all adducts.

cm^{-1} in the reaction coordinate. CP$_2$ is the compound considered as product complex in the pathway that can be decomposed to CH$_3$NH$_2$, OH and O$_2$. The decomposition is results from breaking of 8N-1O, 1O-3O bonds, directly, without entrancing into any transition state. As we know, the ground state of the O$_2$ is a triplet state, subsequently, the CH$_3$NH + OH+^{1}O$_2$, as a product of this channel is metastable and it can be converted to CH$_3$NH + OH +^{3}O$_2$ by the spin relaxation procedure and produce ^{3}P$_2$. In figure 2, relaxation pathway of ^{1}O$_2$ to ^{3}O$_2$ is shown by dashed line rather than the solid line.

In path P$_2$ (2), formation of IN1 is similar to path P$_1$. IN1 is transformed into CP$_2$ via TS4 with an energy barrier of 41.79 kcal/mol. Imaginary frequency of TS4 is 199i cm^{-1}. TS4 has a four-membered ring structure. This structure undergoes 8N-9H bond rupture transformed into CP$_2$. Formation of ^{3}P$_2$ from CP$_2$ is similar to path P$_2$ (1).

3.2b *Formation pathway of P$_2$*: For product P$_2$ (CH$_3$NH + OH + ^{3}O$_2$), there are two possible pathways.

$$\text{Path P}_2(1): \text{R} \rightarrow \text{C}_1 \rightarrow \text{CP}_2 \rightarrow \text{P}_2$$

$$\text{Path P}_2(2): \text{R} \rightarrow \text{C}_1 \rightarrow \text{IN1} \rightarrow \text{CP}_2 \rightarrow \text{P}_2$$

In path P$_2$ (1), C$_1$ as an initial complex undergoes 10H-3O bond formation and 8N-10H bond rupture. This leads to the formation of product complex denoted as CP$_2$ via TS5 with an energy barrier of 29.04 kcal/mol. Imaginary frequency of TS5 is 1011i

3.2c *Formation pathway of P$_3$ (NH$_2$CH + HO$_2$+ OH)*: For product P$_3$, there is only one possible pathway.

$$\text{Path P}_3: \text{R} \rightarrow \text{C}_1 \rightarrow \text{IN1} \rightarrow \text{IN3} \rightarrow \text{CP}_4 \rightarrow \text{CP}_3 \rightarrow \text{P}_3$$

Formation of IN3 is similar to path P$_1$. IN3 undergoes 6H-10O bond rupture and 6H-9O bond formation to transform into CP$_4$ via TS6 with an energy barrier of -27.36 kcal/mol and imaginary frequency of 356i cm^{-1} in the reaction pathway. TS6 has a five-membered ring structure that is formed when the amine H atoms of CH$_3$NH$_2$ approach two terminal atoms of ozone

molecule. CP_4 is transformed into CP_3 via TS7 with an energy barrier of 23.79 kcal/mol. Imaginary frequency of TS7 is 790i cm^{-1}. CP_3 is the complex between OH, NH_2CH and HO_2. It can be directly decomposed to OH, HO_2 and NH_2CH by 1C-3H and 8O-10O bond rupture, without any transition state.

3.2d *Formation pathway of P4 ($^1CH_2NH +^1 H_2O +^3O_2$):*

For product P_4, there is only one possible pathway.

Path P_4 : R → C_1 → IN1 → IN3 → CP_4 → P_4

Formation of CP_4 is similar to path P_3. CP_4 is the complex between H_2O, CH_2NH and $^1O_2$. It can be directly decomposed to $H_2O + CH_2NH + ^1O_2$ by 5N-6H and 10O-8O bonds rupture. Singlet molecular oxygen is metastable, as we know, $^1O_2$ can be relaxed into the triplet molecular and $^3P_4$ produced. $^3P_4$ is 30.24 kcal/mol lower than $^1P_4$.

3.2e *Formation pathways of P_5 and P_6:*

There is only one pathway to reach P_5 and only one pathway to reach P_6.

Path $P_5(1)$: R → C_1 → IN2 → CP_6 → CP_5 → P_5

Path $P_5(2)$: R → C_1 → IN2 → CP_6 → P_6
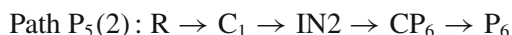
C1 undergoes 6H-2O and 4C-3O bond formation and 4C-6H bond rupture to form IN2 via TS8 with an energy barrier of 15.61 kcal/mol. IN2 is 59.55 kcal/mol lower than original reactants ($CH_3NH_2+O_3$).

The intermediate of IN2, is obtained from C_1 via TS8 with imaginary frequency of 1089i cm^{-1}. IN2 is transformed into CP6 via TS9 with an energy barrier of 21.15 kcal/mol and imaginary frequency of 829i cm^{-1} in the reaction coordinate. CP_6 is the complex between three units of NH_3, CH_2O and $^1O_2$. It can be directly decomposed to $NH_3 + CH_2O +^1O_2$ by 8O-9O and 1C-5N and 10O-6H bonds rupture, without any transition state. As we know, the $CH_2O + NH_3+^1O_2$, as final product of this channel is metastable and can be converted to $CH_2O +NH_3+^3O_2$ by the spin relaxation produce $^3P_6$, that is 76.17 kcal/mol less than the original reactants.

For product P_5 ($NH_2CH_2OH+O_2$), CP_6 is transformed to CP_5 via TS10 with the energy barrier of 24.16 kcal/mol. CP_5 is the product complex between $NH_2CH_2OH +^1O_2$, it can be directly decomposed to $NH_2CH_2OH + ^1O_2$ by 4H-10O, 9O-8O bonds rupture without any transition state. According to the above description, $^1P_5$ as a product in this channel is

metastable, therefore, $^1O_2$ is relaxed to $^3O_2$ and $^3P_5$ is produced. $^3P_5$ is 90.04 kcal/mol less than the reactants.

3.3 *Topological analysis of electron density of P_6 as a thermodynamic product*

AIM topological analysis of electron density has been elaborated using the AIM2000 program package. AIM topological analysis has been performed using electron density integrated over atomic basins (up to 0.001 e/bohr^3 level) as well as in terms of electron density, ρ (r), density Laplacian, $\nabla^2\rho$ (r) and bond ellipticity, $\varepsilon = \lambda_1/\lambda_2-1$, at bond critical (BCP), where λ_1 and λ_2 are the eigenvalues of the Hessian of the BCP electron charge density. Application of the atoms and molecules theory to understand the nature of the bonds in greater detail is an interesting approach. This theory is based on the critical points (CP) of the molecular electronic charge density.[20,21] Topological analysis of electronic charge density, ρ (r), and its Laplacian, $\nabla^2\rho$ (r), are used to describe the strength and the characteristic of the bond, respectively. The Laplacian ($\nabla^2\rho$ (r)) is the sum of λ_1, λ_2 and λ_3, where λ_i is the ith eigenvalue of Hessian matrix of the electronic density. If a critical point has two negative and one positive eigenvalue, it is called (3, −1) or the BCP. If a critical point has two positive and one negative eigenvalue, it is called (3, +1) or ring critical point (RCP), which indicates that a ring structure exists.

Topological parameters values for NH_2CH_2OH molecule as an unknown and new species with more relative stability on the CCSD level in atomic units are displayed in table 2. Molecular graph along $CH_3NH_2+ O_3$ reaction in the path $P_5(NH_2CH_2OH+O_2)$ with electronic charge densities and its Laplacian for some important points are plotted in figure 3.

According to the theory of AIM, the Laplacian of the electron density ($\nabla^2\rho$ (r)) describes the characteristic of the bond. In general, when $\nabla^2\rho$ (r) < 0, the bond is covalent, but when $\nabla^2\rho$ (r) > 0, the bond belongs to the electrostatic interaction. The Laplacian of electronic charge densities values for various bonds of NH_2CH_2OH molecule in table 2 indicat that all bonds in this species have covalent character. Electronic charge density analysis shows that the O-H bond is stronger than the others bonds in NH_2CH_2OH. Ellipticity is a measure of the ratio of the rate of density decrease in the two directions perpendicular to the bond path at the bond critical point, the general shape of the bond and the degree of π-character. Values for ellipticity of $P_5(NH_2CH_2OH+O_2)$ are listed in table 2.

Table 2. Topological analyses of NH$_2$CH$_2$OH molecules on the RB3LYP level; values are in atomic units.

| Bond | P | Eigen of the Hessian matrix | | | $\nabla^2 \rho$ | ε |
		λ_1	λ_2	λ_3		
C-N	0.2849	−0.6126	−0.5869	0.3855	−0.8140	0.04364
C-H	0.2922	−0.8281	−0.8024	0.5505	−1.0801	0.03207
C-H	0.2880	−0.8138	−0.7880	0.5551	−1.0466	0.03273
H-O2	0.1251	−0.3477	−0.3264	0.657	−0.0171	0.06525
O-H	0.3742	−1.9603	−1.9215	0.9272	−2.9546	0.02019
C-O	0.2653	−0.5853	−0.5135	0.4586	−0.4602	0.1398
N-H1	0.3501	−1.3289	−1.2685	0.8552	−1.7422	0.04761
N-H2	0.3510	−1.3256	−1.2594	0.8600	−1.7250	0.05259

Table 3. Thermodynamic data for CH$_3$NH$_2$+O$_3$ reaction on the singlet potential energy profile at the RB3LYP method (kcal/mol).

Species	ΔE^0	ΔH^0	ΔG^0	TΔS^0
CH$_3$NH$_2$+O$_3$ →CH$_3$NO+H$_2$O$_2$	−48.32	−48.32	−48.88	0.56
CH$_3$NH$_2$+O$_3$ →CH$_3$NH+OH+^{3}O$_2$	9.93	10.53	0.281	10.25
CH$_3$NH$_2$+O$_3$ →NH$_2$CH+HO$_2$+OH	29.27	29.86	19.16	10.70
CH$_3$NH$_2$+O$_3$ →CH$_2$NH+H$_2$O+^{3}O$_2$	−76.30	−74.20(−63.34)	−84.32	10.11
CH$_3$NH$_2$+O$_3$ →NH$_2$CH$_2$OH+^{3}O$_2$	−83.73	−83.73	−82.84	−0.89
CH$_3$NH$_2$+O$_3$ →CH$_2$O+NH$_3$+^{3}O$_2$	−76.87	−76.26(−67.16)	−86.71	10.44(8.06)

Experimental values in parentheses are obtained from ref.[22]

3.4 *Thermodynamic data in the CH$_3$NH$_2$+ O$_3$ reaction process*

Change in thermodynamic characteristics for each reaction channel is the difference between the corresponding thermodynamic properties of the products and reactants. Frequency analysis shows that the zero-point-energy (ZPE) of the reactants, intermediates, transition states and products is large. So, the thermodynamic data is corrected by ZPE for CH$_3$NH$_2$+ O$_3$ reaction. Relationships of thermodynamics properties are as follows

$$\Delta E^0 = E_{el} + ZPE, \quad (1)$$
$$\Delta G^0 = \Delta H^0 - T\Delta S^0. \quad (2)$$

Here, ΔE^0 is the standard internal energy of reaction, E_{el} is the total electronic energy and ZPE is zero point energy. The calculated relative internal energies, enthalpies, Gibbs free energies and entropies of all steps in the reactions of gas phase at atmospheric pressure and temperature of 298.15 K, are summarized in table 3. Table 3 shows that ΔH^0 and ΔG^0 for products of P$_1$, P$_4$, P$_5$, and P$_6$ are negative which means that the reactions are exothermic and spontaneous. These values for P$_2$ and P$_3$ paths are positive which means that reactions

are endothermic and non-spontaneous. P$_6$ is a thermodynamic product for having the most negative ΔG^0 in the reaction CH$_3$NH$_2$+ O$_3$.

4. Conclusions

Our theoretical study leads to the following conclusions.

1. Details of the atmospheric oxidation reaction of CH$_3$NH$_2$ with ozone on the singlet PEP were characterized using RB3LYP and CCSD(T) level of computation in connection with the 6-311++G(3df-3pd) basis set.
2. Different structures corresponding to various stationary points on the potential energy profile and transition states were optimized.
3. Six kinds of products are obtained from one reactant complex; four of them have enough thermodynamic stability. Results reveal that the P$_6$ adduct is thermodynamically the most stable product in comparison to others.
4. P$_2$ product with one low-level transition state is the most favoured adduct from a kinetic viewpoint.

Supplementary Information

Cartesian coordinate and frequencies of the reactants, products, intermediates and transition states involved in the $CH_3NH_2+ O_3$ reaction at the RB3LYP/6-311+G(3df-3pd) level of theory are collected in the supplementary data. For details, see www.ias.ac.in/chemsci.

References

1. Mitchell S C and Zhang A Q 2001 *Clin. Chim. Acta* **312** 107
2. Corbin D, Schwarz S and Sonnichsen G 1997 *Catal. Today* **37** 71
3. Huerta F, Morallon E, Perez J M, Vazquez J L and Aldaz A 1999 *J. Electroanal. Chem.* **469** 159
4. Tian W, Wang W, Zhang Y and Wang W 2009 *Int. J. Quantum. Chem.* **109** 1566
5. Liua J, Lva C, Guoa Y and Wangb G 2013 *Appl. Surf. Sci.* **271** 291
6. http://pubchem.ncbi.nlm.nih.gov/summary/summary.cgi?sid$=$3518#x351.
7. Li X, Meng L and Zhang S 2007 *J. Mol. Struct.* **847** 52
8. Alhambra C, Sanchez M L, Corchado J C, Gao J and Truhlar D G 2002 *Chem. Phys. Lett.* **355** 388
9. Kaye J A and Strobel D F 1983 *ICARUS* **55** 399
10. Zhu S, Li Q, Dua Y, Yang X, Fan J and Dong Z 2010 *Toxicol. In Vitro* **24** 809
11. Chintharlapalli S, Papineni S, Baek S J, Liu S and Safe S 2005 *Mol. Pharmacol.* **68** 1782
12. Peel J B and Willett G D 1975 *J. Chem. Soc. Faraday Trans. II* **71** 1799
13. Tiwary S and Mukherjee A 2009 *J. Mol. Struct.: THEOCHEM* **3** 57
14. Zhang L, Liu H, Tang H and Huang T 2014 *Chem. Pap.* **68** 145
15. Kayi H, Kaiser R and Head J 2011 *Phys. Chem. Chem. Phys.* **13** 11083
16. Frisch M J, Trucks G W, Schlegel H B, Scuseria G E, Robb M A, Cheeseman J R, Montgomery J A Jr, Vreven T, Kudin K N, Burant J C, Millam J M, Iyengar S S, Tomasi J, Barone V, Mennucci B, Cossi M, Scalmani G, Rega N, Petersson G A, Nakatsuji H, Hada M, Ehara M, Toyota K, Fukuda R, Hasegawa J, Ishida M, Nakajima T, Honda Y, Kitao O, Nakai H, Klene M, Li X, Knox J E, Hratchian H P, Cross J B, Adamo C, Jaramillo J, Gomperts R, Stratmann R E, Yazyev O, Austin A J, Cammi R, Pomelli C, Ochterski J W, Ayala P Y, Morokuma K, Voth G A, Salvador P, Dapprich S, Daniels A D, Strain M C, Farkas O, Malick D K, Rabuck A D, Raghavachari K, Foresman J B, Oritz J V, Cui Q, Baboul A G, Clifford S, Stefanov B B, Liu G, Liashenko A, Piskorz P, Komaromi I, Martin R L, Fox D J, Peng C Y, Nanayakkara A, Challacombe M, Gill P M W, Johnson B, Chen W, Wong M W, Gonzalez C and Pople J A 2003 Gaussian 03, Revision B.03. Gaussian Inc., Pittsburgh, PA
17. Becke A D 1993 *J. Chem. Phys.* **98** 1372
18. Lee C, Yang W and Parr R G 1988 *Phys. Rev.* **B37** 785
19. Biegler-Kning F 2000 AIM2000 Ver 1.0. University of Applied Science, Bielefeld, Germany
20. Bader R F W 1990 *Atoms in molecules – a quantum theory* (Oxford: Oxford University Press)
21. Bader R F W 1991 *Chem. Rev.* **91** 893
22. NIST Chemistry WebBook, NIST Standard Reference Database Number 69, www.nist.gov.